

Physicochemical characterization of chitosan nanoparticles: electrokinetic and stability behavior

T. López-León^a, E.L.S. Carvalho^b, B. Seijo^b, J.L. Ortega-Vinuesa^a, D. Bastos-González^{a,*}

^a *Biocolloid and Fluid Physics Group, Department of Applied Physics, University of Granada, Av. Fuentenueva S/N, 18071 Granada, Spain*

^b *Department of Pharmacy and Pharmaceutical Technology, School of Pharmacy, University of Santiago de Compostela, 15706 Santiago de Compostela, Spain*

Received 5 January 2004; accepted 30 August 2004

Available online 7 December 2004

Abstract

Some physical properties of nanogel particles formed by chitosan ionically cross-linked by tripolyphosphate (TPP) have been studied. Electrokinetic properties and colloidal stability were analyzed as a function of pH and ionic strength of the medium. Chitosan particles showed volume phase transitions (swelling/shrinking processes) when the physicochemical conditions of the medium were changed. Experimental data were mainly obtained by electrophoretic mobility measurements and by photon correlation spectroscopy and static light scattering techniques. Chitosan chains possess glucosamine groups that can be deprotonated if the pH increases. Therefore, modification of pH from acid to basic values caused a deswelling process based on a reduction of the intramolecular electric repulsions inside the particle mesh. Electrophoretic mobility data helped to corroborate the above electrical mechanism as responsible for the size changes. Additionally, at those pH values around the isoelectric point of the chitosan–TPP particles, the system became colloiddally unstable. Ionic strength variations also induced important structural changes. In this case, the presence of KCl at low and moderate concentrations provoked swelling, which rapidly turned on particle disintegration due to the weakness of chitosan–TPP ionic interactions. These last results were in good agreement with the predictions of gel swelling theory by salt in partially ionized networks.

© 2004 Elsevier Inc. All rights reserved.

Keywords: Electrophoretic mobility; Colloidal stability; Gel phase transitions; Chitosan nanoparticles

1. Introduction

The potential use of polymeric nanoparticles as drug carriers has led to the development of many different colloidal delivery vehicles. The main advantages of this kind of systems lie in their capacity to cross biological barriers, to protect macromolecules, such as peptides, proteins, oligonucleotides, and genes from degradation in biological media, and to deliver drugs or macromolecules to a target site with following controlled release. In the last years several synthetic as well as natural polymers have been examined for pharmaceutical applications. A basic requirement for these polymers to be used in humans or animals is that

they have to degrade into molecules with no toxicity for biological environments. For this biocompatibility reason, a very limited numbers of polymers can be used to prepare biodegradable materials. Recently, natural chitosan material has attracted great attention in pharmaceutical and biomedical fields [1–3] because of its advantageous biological properties, such as biodegradability, biocompatibility, and nontoxicity. Chitosan is a cationic polysaccharide obtained by partial deacetylation of chitin, the major component of crustacean shells. In contrast to other polymers, chitosan is a hydrophilic polymer with positive charge that comes from weak basic groups, which give it special characteristics from the technological point of view. K.A. Janes et al. [4] have published an extensive paper where the current state of the art of the specific features and applications of the chitosan-based nanoparticles as systems for delivery macromolecules is reviewed.

* Corresponding author. Fax: +34-958-243214.

E-mail address: dbastos@ugr.es (D. Bastos-González).

Two different techniques are usually employed to obtain chitosan microparticles: On the one hand, chitosan chains can be chemically cross-linked leading to quite stable matrixes, where the strength of the covalent bonds stands out. Glutaraldehyde is broadly used as a cross-linking molecule in covalent formulations. On the other hand, chitosan hydrogels can be also obtained by ionic gelation, where micro- or nanoparticles are formed by means of electrostatic interactions between the positively charged chitosan chains and polyanions employed as cross-linkers. The most extensively used polyanion is the tripolyphosphate (TPP). Due to the proved toxicity of glutaraldehyde and other organic molecules used in the synthesis of gels covalently stabilized, only the second synthesis technique (ionic gelation) can be used for pharmaceutical applications.

In spite of the important effort that is still being made to develop suitable systems based on chitosan chemistry that allow delivery of new macromolecules, very few studies include a complete physicochemical characterization of them. It is worth remarking that the physicochemical properties not only affect the absorption and release processes but also govern the interaction of the particles with different biological compounds (proteins or membranes) of the tissue where they are introduced. Accordingly, the success in the development of the polymeric particles acting like delivery vehicles is determined by a detailed knowledge of their chemical nature and physical properties which would explain how they interact with their biological environment. This lack of information on chitosan–TPP particles may be caused by their labile structure, which easily disintegrates when conditions of the medium where they are immersed change. It must be noted that there are publications dealing with physicochemical characterization of chitosan gels, but they are usually focused on macroscopic films [5,6], microspheres obtained by covalent cross-linking [7,8], and nanoparticles achieved by direct precipitation of chitosan chains in absence of cross-linking molecules [9]. Chitosan nanogels synthesized by ionic gelation with TPP has been analyzed indeed [10–12], but the studies have been mainly paid to those features related to their drug delivery and release properties. Thus, the goal of this work deals with the characterization of physical properties related to swelling/shrinking patterns, electrical properties, colloidal stability and phase transitions of this kind of chitosan–TPP nanogels. Such a characterization is supported by theoretical approaches.

One of the most important properties of any nanogel is the extent of swelling [13]. This means that its structure can undergo volume phase transitions from swollen to collapsed states. As an example, this feature is extremely important from the applicability point of view, since the deliver and release capacity of the particles significantly changes from a swollen to a collapsed state. The extent of swelling depend on several external conditions such as the temperature, pH or ionic strength of the medium. Experimental data are usually obtained from changes in the hydrodynamic diameters measured by photocorrelation spectroscopy (PCS) [14]. Another

essential aspect to take into account is the colloidal stability of the particles when they are immersed in media with conditions of ionic strength and pH similar to those found in biological environments. Aggregation of these soft particles has also been analyzed using PCS techniques. The stability of the systems depends, to a great extent, on the electrical state of the nanoparticles [15]. In the absence of steric stabilization mechanisms, information on the electrical properties of the system helps to explain aggregation features. Such information can be obtained from electrophoretic mobility data, which not only can corroborate the colloidal stability data, but also can cast some light on swelling–shrinking processes [16].

2. Experimental

2.1. Reagents

All the salts employed in this work were of analytical grade and purchased from different firms: Sigma, Pan-reac, and Scharlau. Two sorts of buffers were used: anionic buffers were prepared with solutions of acetate (pH 4 and 5), phosphate (pH 6 and 7), and borate (pH 8, 9, and 10); cationic buffers were used for buffering pH 6 and 7 (bis–tris), pH 8 and 9 (tris), and pH 10 (AMP, 2-amino-2-methyl-1-propanol). All the buffered solutions had an ionic strength equal to 2 mM. Chitosan in the form of hydrochloride salt (Protasan 110 Cl, $M_n > 50$ kDa, deacetylation degree 87%) was purchased from Pronova Biopolymer (Norway). Pentasodium tripolyphosphate (TPP) was supplied by Sigma. Double-distilled and deionized water was used throughout.

2.2. Preparation of chitosan nanoparticles

Nanoparticles were produced based on ionic gelation of tripolyphosphate (TPP) and chitosan as described elsewhere [10]. Nanoparticles were spontaneously obtained upon the addition of 1.2 ml (0.84 mg/ml, w/v) of a TPP aqueous basic solution to 3 ml of the chitosan acidic solution (2 mg/ml, w/v) under magnetic stirring at room temperature. Nanoparticles were concentrated by centrifugation at 16,000g in a 10- μ l glycerol bed for 30 min. The supernatants were discarded and nanoparticles resuspended in water with 5% trehalose for further freeze-drying (Labconco, Kansas City, MI, United States) under the following conditions: a primary drying step for 48 h at -30 °C and a secondary drying step until the temperature gradually rose to $+20$ °C.

2.3. Electrophoretic mobility

Electrophoretic mobility measurements were performed with a Zeta-Sizer IV (Malvern Instruments). Chitosan particles were diluted in the desired buffer or electrolyte solution to obtain a final chitosan concentration equal to 10.2 mg/l.

Data were obtained from the average of six measurements at the stationary level in a cylindrical cell. Standard deviation was always lower than 5%.

2.4. Size, swelling, and stability studies

The average size of the particles was determined by photon correlation spectroscopy (PCS) with a commercial light-scattering setup, 4700C, Malvern Instruments, Malvern, UK, with an argon laser of wavelength $\lambda_0 = 488$ nm. PCS makes it possible to calculate the average diffusion coefficient (D) of the particles. Assuming that the particles are solid, the mean diameter (d) can be easily calculated by the Stokes–Einstein equation,

$$d = \frac{kT}{3\pi\eta D}, \quad (1)$$

where k is the Boltzmann constant, T is the absolute temperature, and η is the viscosity of the medium. It should be noted that sizes given in the figures of this paper are slightly overestimated, as soft particles possess lower D than hard ones due to frictional reasons. Previously, to carry out the measurements, the best experimental conditions were investigated and set at the following values: laser power = 33 mW; particle concentration per volume unit = 10^{-3} ; and measurement angle = 90° . Volume phase transitions induced by adding salt were simultaneously studied by static light scattering (SLS) and PCS using the same optical instrument.

3. Results and discussion

3.1. Destabilization of chitosan nanoparticles during storage

Chitosan degrades with time in the presence of enzymes (i.e., lysozyme) when inserted into biological environments [17]. However, we have also found that chitosan nanoparticles synthesized by ionic gelation lose their integrity in aqueous media even in the absence of enzymes. Chitosan–TPP particles were incubated in a nonbuffered and low-ionic-strength solution (1 mM in KBr) in order to analyze the possible degradation of the system. Three chitosan aliquots were stored at different temperatures, -10°C , 5°C , and room temperature (22°C , approximately). Then the particle sizes were measured as a function of time through 1 month. The freezing and subsequent melting process carried out with the -10°C sample induced complete destabilization of the system. Therefore, the system becomes absolutely useless and it must be discarded for any application. Results obtained with the 5 and 22°C aliquots are shown in Fig. 1. In both cases, it can be seen that particle sizes and standard deviations increased with time. This can be explained if chitosan nanoparticles erode, losing their spherical shape, in an aqueous environment.

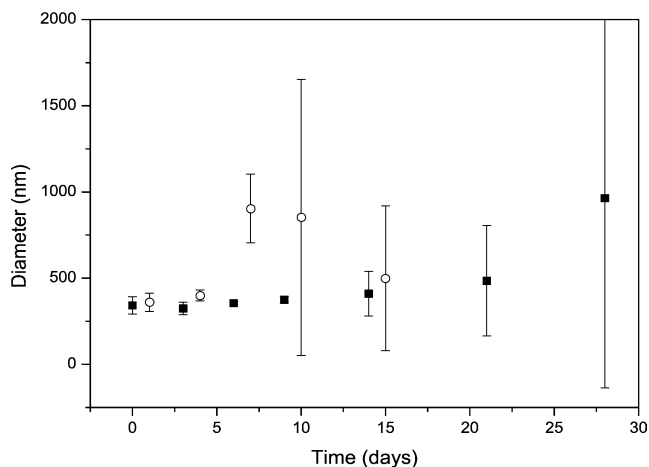


Fig. 1. Average diameter of chitosan nanoparticles stored at 5°C (■) and 22°C (○) as a function of time. Incubated in a nonbuffered solution (pH in the range 5–6) containing 1 mM of KBr.

This conformational change modifies the diffusion coefficient of the particles, increasing it. As a consequence the mean diameter also rises. Moreover, polydispersity increments due to the lack of sphericity bear a high uncertainty in the measurements. Fig. 1 also shows that the pool stored at room temperature degraded much quicker than that stored in the refrigerator. Anyway, none of the two samples showed good stability, since the average size and its standard deviation began to increase significantly after 15 and 7 days for 5 and 22°C samples, respectively. Such spontaneous disintegration takes place under very mild conditions. This suggests that chitosan–TPP nanogels behave as a metastable system, and thus, they must be stored lyophilized, and fresh aqueous solutions only prepared when required.

3.2. Electrophoretic mobility studies

In order to obtain information about the electrical state of the ionizable groups of the chitosan–TPP particles, electrophoretic mobility (μ_e) was measured as a function of pH and salt concentration.

As no previous studies exist with these kind of systems, the stabilization time of the electrical double layer (e.d.l.) and suitable particle concentrations were first investigated to ensure reliable and reproducible μ_e data in the rest of the experiments. Fig. 2a shows the results of μ_e versus waiting time. It can be seen that formation of a stable e.d.l. is not instantaneous; a relaxation time exists. This is due to the time it takes the electrolyte ions to interpenetrate toward the particle nucleus. The μ_e remained constant after 25 min. Therefore, 30 min were always waited before beginning to measure the μ_e of any chitosan particle solution. On the other hand, as the device used to measure the mobility is based on light scattering, it also becomes important to optimize the number of particles to obtain accurate μ_e measurements. Fig. 2b shows the μ_e as a function of chitosan particle concentration. It can

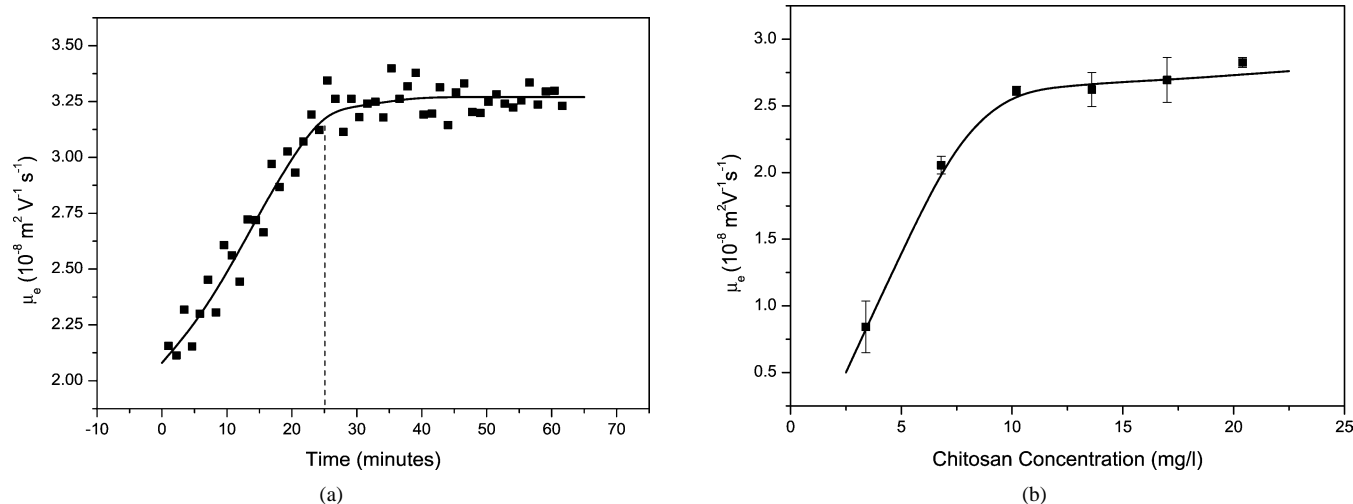


Fig. 2. Electrophoretic mobility as a function of (a) time and (b) particle concentration.

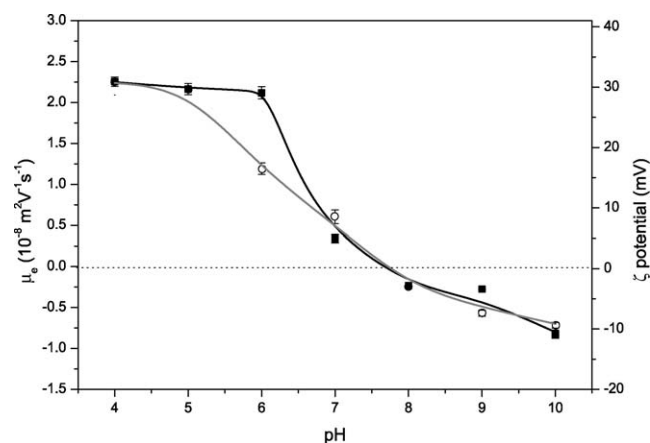


Fig. 3. Electrophoretic mobility as a function of pH of the medium. Anionic buffers (○) and cationic buffers (■).

be seen that mobility remained constant from 10 mg/l. So this concentration value was chosen for carrying out the rest of the experiments.

The pH effect on the μ_e of chitosan particles was then studied. Anionic and cationic buffers of low ionic strength (2 mM) covering the pH range from 4 to 10 were selected to test if the salts used in the buffers somehow affected the μ_e data. Chitosan tends to form ion pairs with nonmonovalent anions, a property which is broadly used in ionic gelation processes by using tripolyphosphate [10–12] or sulfate [18,19] as cross-linking molecules. Therefore, the presence of phosphate or borate may affect some chitosan properties. Fig. 3 shows the obtained results. The nature of the buffering salts did not give significant differences in the μ_e , except at pH 6, where the anionic buffer (phosphate) showed a considerable reduction of the μ_e value compared with the cationic one. Something similar happened at pH 9 (borate), but this difference was not so important. Cationic buffers seemed to be more appropriate, since undesired buffer–chitosan electrostatic interactions are avoided. To verify this, chitosan

$\text{p}K_a$ values were obtained. There is a simple procedure to calculate the $\text{p}K_a$ from data shown in Fig. 3 based on the following equation [20,21],

$$\text{p}K_a = \text{pH}_{\zeta=\zeta_{\text{plateau}}/2} \pm \frac{0.4343F\zeta_{\text{plateau}}}{2RT}, \quad (2)$$

where $\text{pH}_{\zeta=\zeta_{\text{plateau}}/2}$ is the pH where the maximum value of the zeta potential “ ζ_{plateau} ” is reduced by half. The “+” sign is used for particles with weak acid groups, whereas the “–” is for weak basic ones. F , R , and T have the usual meaning. The $\text{p}K_a$ values thus obtained were 6.3 and 5.7 for cationic and anionic buffers, respectively. Only the former lay in the $\text{p}K_a$ range reported for chitosan, which usually goes from 6 to 7, depending on their deacetylation degree and the global dissociation constant of glucosamine groups [9]. So the cationic buffers seem not to interfere in the chemical properties of chitosan, whereas the anionic ones show some specific interactions.

It can be also seen in Fig. 3 that chitosan–TPP complexes presented an isoelectric point (i.e.p.) around 7.5. The inversion in the mobility sign at basic pH is given by the tripolyphosphate ionic groups, since at those pH the glucosamine groups of chitosan are practically uncharged. It is also observed that μ_e was higher, in absolute value, when particles are positive than when they are negative. This was expected, as chitosan is a highly charged polymer below its $\text{p}K_a$. Surprisingly, the mobility values were rather low even at acid pH, at which chitosan chains are totally protonated. This could be justified by the soft nature of our nanogel particles. The mobility is a result of the competition between variations in charge density and friction coefficient [16]. Frictional forces become more significant in swollen gels than in compact ones. The more charge density, the more swelling state, and thus higher friction during particle motion. In addition to frictional forces, there would be another explanation based on ion condensation mechanisms [22], which appear in highly charged particles. More-

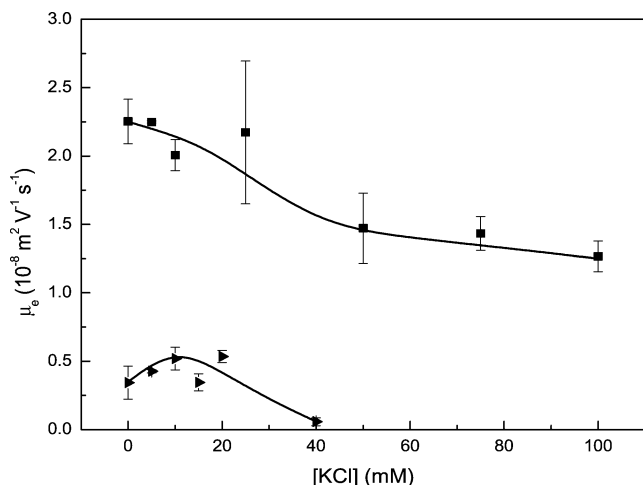


Fig. 4. Electrophoretic mobility as a function of KCl concentration at pH 4 (■) and pH 7 (▴).

over, it should be also noted that some positive charges of chitosan are canceled by negative TPP groups.

Finally, the mobility was measured as a function of KCl concentration. Results are shown in Fig. 4. The μ_e values were obtained at two different pHs. One set was buffered at pH 4 and another at pH 7, at which the net charge of the particles is still positive but close to zero. Two features can be observed: (i) μ_e values were much greater at pH 4 than at pH 7; this result was expected, taking into account the charge differences among the nanoparticles at both pHs. (ii) Mobility diminished for increasing KCl concentrations. This pattern is mainly provoked by the double-layer compression, as an increment in salt concentration screens particle charges and thus the mobility decreases [23]. In addition, another effect might contribute. The swelling of partially ionized gels induced by increasing ionic strength is predicted theoretically and observed experimentally [24]. As the frictional forces rise during swelling, they also must induce a reduction in the μ_e values for increasing salt concentrations.

3.3. Swelling and stability behavior

In this section we have analyzed the swelling behavior of chitosan nanogel particles. These volume phase transitions were induced independently by pH and ionic strength changes. The influence of pH will be discussed first.

As the chitosan network contains pH-ionizable groups, a pH variation will modify the network electrical state and thus the swelling behavior. Fig. 5 shows the mean diameter of the particles versus the pH of the medium. The diameter of the nanogels showed a clear tendency to diminish when pH moved from 4 to 7. Therefore, this deswelling behavior is governed by the intramolecular electrostatic contributions. The mobility data shown in Fig. 3 support this explanation. Positive μ_e values decreased to zero for increasing pH, indicating a transition from charged to uncharged gel, which subsequently yields a change in the mesh size. The same

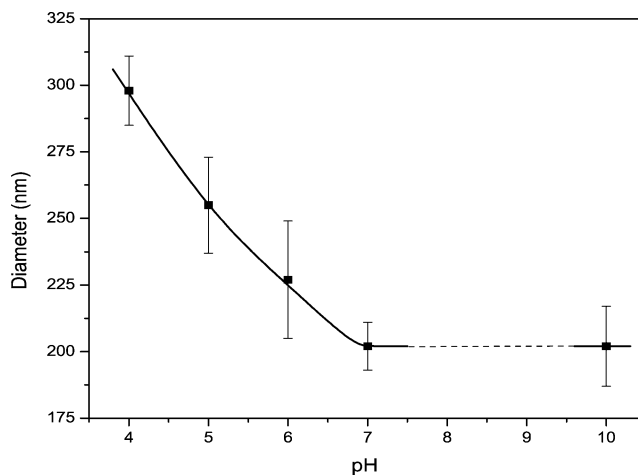


Fig. 5. Mean diameter of the particles as a function of pH.

reasoning can be applied to the pH 10 data, at which particles show negative charge. The μ_e in absolute value was very similar at pH 7 and 10. This would mean similar electrical states at both pHs, although with reversed sign, which would lead to almost identical swelling degrees, as observed. In contrast, a continuous increase of the diameter as a function of time was observed at pH 8 and 9, which indicates aggregation of the system. The mobility data shown in Fig. 3 gave μ_e values rather close to zero at both pHs, suggesting a situation where chitosan–TPP particles exhibit charge cancellation. Fig. 6 shows the diameter evolution as a function of time at pH 9. Identical results were obtained at pH 8. Data at pH 4 have also been included in this figure to underline the different stability behavior between charged and uncharged chitosan–TPP nanogels. The absence of repulsive electrostatic forces affects not only intramolecular but also intermolecular interactions. This makes the system lose its colloidal stability, and thus the uncharged nanospheres start to aggregate. In order to know if this colloidal aggregation by charge cancellation is reversible, an additional experiment was performed. One sample was immersed at pH 8, and the evolution of the mean diameter was recorded for 100 min. Then the pH was changed to 6, adding a small amount (previously calculated) of HCl. Fig. 7 shows the results. It can be seen that after the pH change from basic to acid, the diameter of the particles immediately decreased, reaching a constant average value of 570 nm, approximately. The result indicates that the aggregation process is only partially reversible, as single particles at pH 6 should have an average size equal to 230 nm (see Fig. 5). Therefore, the transition from uncharged (pH 8) to charged gel (pH 6) breaks some aggregates, although it is not capable of rendering the initial single particles.

The most striking results were obtained when KCl was added to inducing colloidal destabilization, keeping the pH constant. Experimental data at pH 4 and pH 7 are plotted in Figs. 8a and 8b, respectively. Note that information of two parameters were simultaneously collected by the optical device, the average diameter of the particles obtained by PCS

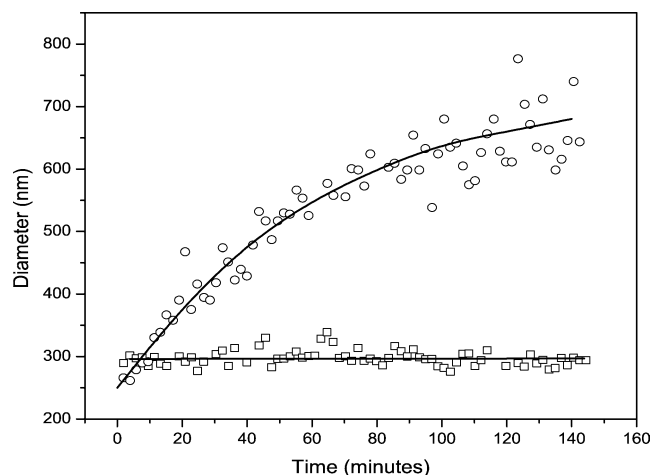


Fig. 6. Kinetic evolution of the mean diameter of aggregates when immersed at pH 4 (□) and 9 (○).

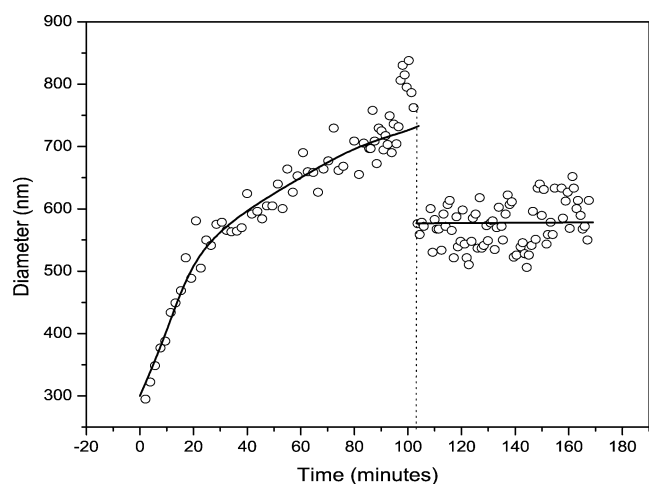


Fig. 7. Kinetic evolution of the mean diameter of aggregates immersed at pH 8 and monitored for 100 min; then the pH was changed to 6.

and the light intensity scattered by the sample measured by SLS. No kinetics was evaluated in this set of experiments, as measurements were only taken from samples in stationary or equilibrium states. It is worth highlighting that no clear aggregation was found; in contrast, a sharp decrease in the intensity of the scattered light was observed. Particle diameters only increase initially, pass through a maximum, and then decrease. Meanwhile, the scattered light intensity linearly decreases before a constant value is obtained which coincides with that obtained with a blank (pure solvent). This is a surprising result that suggests that chitosan–TPP particles disintegrate in the presence of low or moderate salt concentrations. There is another feature associated with the size changes. At pH 4 the initial diameter increment is small, whereas that observed at pH 7 is notable (see axes scales). In order to be able to explain all these results some theoretical points related to gel swelling by salt effects have been considered.

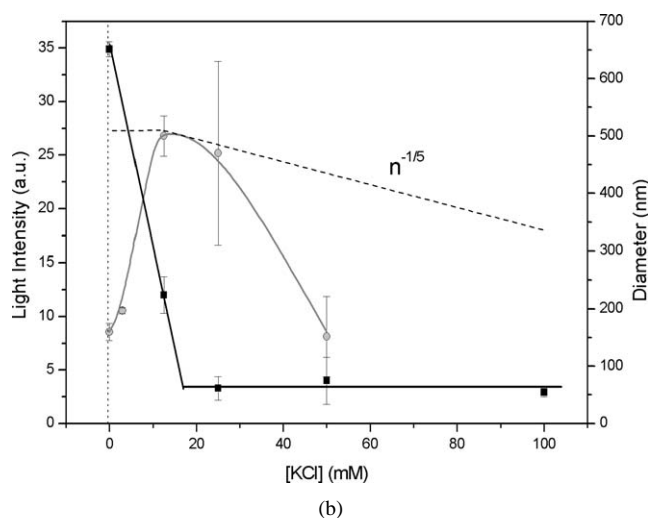
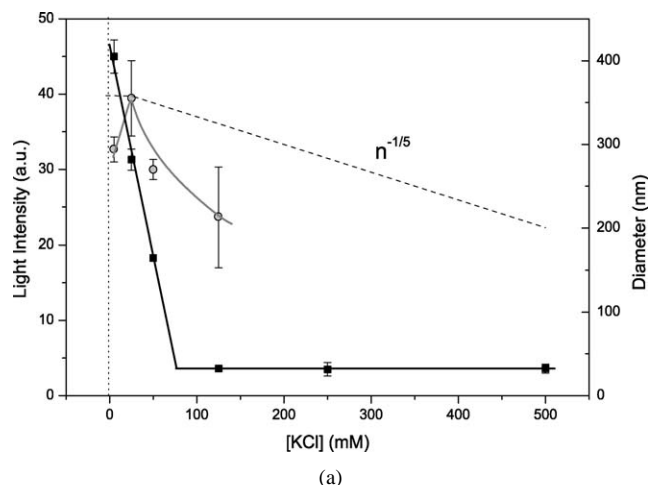


Fig. 8. Intensity of the scattered light (■) and mean diameter (○) of chitosan particles at (a) pH 4 and (b) 7, as a function of KCl concentration. Dashed line corresponds to the theoretical $d \sim n^{-1/5}$ dependence.

The macroscopic state of a homogeneous neutral gel is commonly described by the Flory–Huggins thermodynamic theory, which is based on solvent–polymer interactions and elastic contributions of the network [25]. According to this theory, thermodynamic equilibrium for a gel is attained when the chemical potential of the solvent is equal inside and outside the gel, that is, when no transfer of solvent takes place across the gel–solvent interface. Thus, once equilibrium is reached, the net osmotic pressure in a gel must be zero. For good solvents, the osmotic mixing pressure would tend to swell the particle, while the elastic contribution would act to shrink the gel. In equilibrium both forces are balanced. However, for ionic gels, additional osmotic contributions given by the solved ions must be taken into account through the Donnan theory [26], which predicts an unequal distribution of ions inside and outside the charged gel.

For the sake of clarity and in order to better analyze the salt effect in phase transitions, the mixing contribution will be neglected, which is a good approximation in our experi-

mental conditions [16]. Therefore, the gel size will be controlled by the competition between elastic and ionic terms.

The elastic term (π_e) is given by Flory theory [26] as

$$\pi_e = \frac{N_C k T}{V_0} \left[\frac{1}{2} \left(\frac{d_0}{d} \right)^3 - \frac{d_0}{d} \right], \quad (3)$$

where N_C is the effective number of chains of the network, k the Boltzmann constant, T the absolute temperature, and V_0 the gel volume in the collapsed state. The symbols d_0 and d stand for the diameters of the particles in the collapsed and swollen states, respectively.

The ionic term (π_i) is given by Donnan theory [26],

$$\pi_i = N_A k T \sum_i (n_i - n_i^*), \quad (4)$$

where N_A is the Avogadro number and n_i and n_i^* refer to the concentration of the i -ionic species inside and outside the gel, respectively. When the bulk salt concentration, n , is smaller than the counterion concentration inside the gel, π_i is independent on salt concentration. In contrast, π_i depends on n^{-1} for high ionic strengths [27].

By balancing the above two equations ($\pi_e + \pi_i = 0$), the theoretical diameter dependence of charged microgel particles on salt concentration is null for low ionic strengths and linear in $n^{-1/5}$ for high concentrations. None of these predicted patterns are, however, observed in Figs. 8a and 8b. First, an initial increment in the particle diameter was observed as salt concentration increased. The swelling yielded by an increment in electrolyte concentration is a process also predicted theoretically, provided that gels are partially ionized. Fernández-Nieves et al. [16] demonstrated that the addition of salt modifies the ionic distribution inside the gel, altering the number of dissociated groups in the network, and then changing the net charge. This modification in the network electrical state makes particles swell or shrink, depending on whether the electrical repulsions increase or decrease, respectively. These authors showed both theoretical and experimental swelling processes for moderate increments of ionic strength. At higher ionic strengths the swelling stopped, the mean diameter reached a maximum and then diminished according to $n^{-1/5}$ in a gel covalently synthesized. As mentioned, the swelling by salt is expected in partially ionized networks. Our chitosan particles absolutely fulfill this condition at pH 7. At this neutral pH the size increment was more significant than that observed at pH 4, at which chains should be totally ionized.

On the other hand, the linear behavior in $n^{-1/5}$ is a universal dependence, provided that microgel particles keep their own entity. The size of our samples rapidly diminished once the maximum was reached, going away from the theoretical linear behavior. This peculiar feature, together with the light intensity data, allows us to conclude that the particles disappear by salt effects. As the intensity of scattered light rapidly decreases, and considering that electrostatic interactions between chitosan chains and TPP molecules can

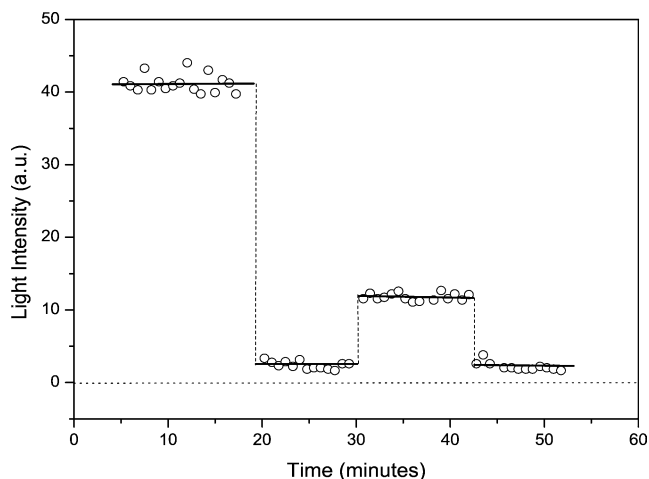


Fig. 9. Intensity of the light scattered by chitosan particles at pH 4 when ionic strength was alternatively changed from 25 (KCl) to 125 mM. The first data correspond to KCl 25 mM, and the last to 125 mM.

be insufficient to withstand the osmotic pressure, disintegration of particles is considered as a plausible process. A long time ago, Breitenbach and Karlinger [28] also observed disintegration during swelling, even in gels covalently stabilized. Disintegration takes place at lower KCl concentrations in pH 7 than in pH 4. At neutral pH chitosan chains are partially uncharged, and thus the electrical interactions with TPP become weaker. This makes particles rapidly lose their entity as soon as they start to swell.

Despite all the experimental data having been qualitatively supported by a theoretical treatment, there are two points that can be controversial. First, the size increase observed at pH 7 is rather high if particles only swell by electrostatic intermolecular repulsions, as values over 500 nm in particle diameter are even found. These values are much higher than those expected for completely ionized particles, which must correspond around 300 nm, according to those data shown in Fig. 5 at acid pH. Therefore, the results can only be justified if the addition of salt simultaneously provokes some particle aggregation (predicted by the DLVO theory) together with disintegration induced by swelling. Note that neutral pH is near the i.e.p. of our particles, at which aggregation occurred even in absence of KCl (see Fig. 6). This explanation can be also applied to the second controversial point: at pH 4 (Fig. 8a), the chitosan network is totally ionized according to its pK_a values; the Flory and Donnan theories would not predict any size increase, although a slight increment is observed.

A final experiment was designed in order to corroborate if the disintegration of the particles by adding salt could be a reversible process. Fig. 9 shows initially the light scattered by a sample immersed at pH 4 and containing KCl 25 mM. Then the salt concentration was increased to 125 mM, and this instantaneously triggered disintegration. The system was taken to 25 mM again, and a partial formation of parti-

cles was then observed. These particles rapidly disappeared when the ionic strength was set at 125 mM once more. Only partial reversibility of the system seems to be observed, as the initial light intensity values were not obtained after a 25 → 125 → 25 mM cycle. This pattern can be explained by taking into account that original particles were synthesized in optimal conditions, whereas after disintegration in our last experiment the electrical state of chitosan and TPP together with the medium conditions have been changed. Therefore, the particle disintegration by ionic strength can be considered as an irreversible process.

4. Conclusions

This work shows a systematic study on the chemical physical characterization of gel nanoparticles formed by chitosan chains electrostatically linked by ionic interactions. This kind of particles is of great interest for pharmaceutical applications. The stability, phase transitions, and electrical states of chitosan–TPP particles have been extensively analyzed by means of PCS, SLS, and electrophoretic mobility measurements. These particles have shown extremely labile behavior, where not only aggregation but also disintegration processes occur at environmental conditions easily observed in biological fluids. Although this could make them useless for medical applications, we must emphasize that this is not a general conclusion for chitosan–TPP nanogels containing drugs, genes, or proteins. In fact, this kind of particles have successfully been used as drug delivery systems in human fluids. When the particles are loaded with macromolecules or drugs, the interactions between them and the gel network can effectively make particles much more stable. Contrasting the experimental data with appropriate theories, the following conclusions can also be stated. Changes in pH control the swelling of the particles. The more acid the pH, the bigger diameter is observed, due to intramolecular electrostatic repulsions. Since the pK_a value of the chitosan is close to neutral pH, particles spontaneously aggregate in slightly basic pHs, where they become completely uncharged. Swelling and colloidal aggregation are practically turned to particle disintegration when salt is added, even at moderate concentrations. A swelling mechanism originated by osmotic pressures associated to ionic distributions between the inner part of the gel and the bulk is proposed to explain these last results.

Acknowledgments

The authors thank projects MAT2003-01257 and AGL-2004-01531/ALI from the Comisión Interministerial de Ciencia y Tecnología (CICYT), Spain, for financial support. We are especially indebted to Professor María José Alonso for her comments and suggestions.

References

- [1] V. Dodane, D. Vilivalam, *Pharm. Sci. Technol. Today* 1 (1998) 246.
- [2] W. Paul, C. Sharma, *S.T.P. Pharma Sci.* 10 (2000) 5.
- [3] M.N.V.R. Kumar, *React. Funct. Polym.* 46 (2000) 1.
- [4] K.A. Janes, P. Calvo, M.J. Alonso, *Adv. Drug Del. Rev.* 47 (2001) 83.
- [5] M.N. Khalid, F. Agnely, N. Yagoubi, J.L. Grossiord, G. Couarraze, *Eur. J. Pharm. Sci.* 15 (2002) 425.
- [6] M.-S. Shin, S.I. Kim, I.Y. Kim, N.G. Kim, Ch.G. Song, S.J. Kim, *J. Appl. Polym. Sci.* 84 (2002) 2591.
- [7] X.-X. Tian, M.J. Groves, *J. Pharm. Pharmacol.* 51 (1999) 151.
- [8] T. Banerjee, S. Mitra, A.K. Singh, R.K. Sharma, A. Maitra, *Int. J. Pharm.* 243 (2002) 93.
- [9] C. Schatz, C. Pichot, T. Delair, C. Viton, A. Domard, *Langmuir*, in press.
- [10] P. Calvo, C. Remuñán-López, J.L. Vila-Jato, M.J. Alonso, *J. Appl. Polym. Sci.* 63 (1997) 125.
- [11] K.A. Janes, M.P. Fresneau, A. Marazuela, A. Fabra, M.J. Alonso, *J. Controlled Rel.* 73 (2001) 255.
- [12] A. Vila, A. Sánchez, M. Tobío, P. Calvo, M.J. Alonso, *J. Controlled Rel.* 78 (2002) 15.
- [13] B.R. Saunders, B. Vincent, *Adv. Colloid Interface Sci.* 80 (1999) 1.
- [14] A. Fernández-Nieves, A. Fernández-Barbero, B. Vincent, F.J. de las Nieves, *Langmuir* 17 (2001) 1841.
- [15] J.L. Ortega-Vinuesa, D. Bastos-González, *J. Biomater. Sci. Polym. Ed.* 12 (2001) 379.
- [16] A. Fernández-Nieves, A. Fernández-Barbero, F.J. de las Nieves, B. Vincent, *J. Phys. Condens. Matter* 12 (2000) 3605.
- [17] S.H. Pangburn, P.V. Trecony, J. Heller, in: J.P. Droz (Ed.), *Chitin, Chitosan and Related Enzymes*, Academic Press, New York, 1984.
- [18] A. Berthold, K. Cremer, J. Kreuter, *J. Controlled Rel.* 39 (1996) 17.
- [19] I.M. van der Lubben, J.C. Verhoef, A.C. van Aelst, G. Borchard, H.E. Junginger, *Biomaterials* 22 (2001) 687.
- [20] R.H. Ottewill, J.N. Shaw, *Kolloid Z. Z. Polym.* 218 (1967) 4.
- [21] H.J. Jacobasch, *Angew. Makromol. Chem.* 128 (1984) 47.
- [22] G.S. Maning, *Ber. Bunsen-Ges. Phys. Chem.* 100 (1996) 909.
- [23] R. Hidalgo-Álvarez, A. Martín, A. Fernández, D. Bastos, F. Martínez, F.J. de las Nieves, *Adv. Colloid Interface Sci.* 67 (1996) 1.
- [24] A. Fernández-Nieves, A. Fernández-Barbero, F.J. de las Nieves, *J. Chem. Phys.* 115 (2001) 7644.
- [25] P.J. Flory, *Principles of Polymer Chemistry*, Cornell Univ. Press, London, 1953.
- [26] P.C. Hiemenz, R. Rajagopalan, *Principles of Colloid and Surface Chemistry*, Dekker, New York, 1997.
- [27] J.L. Barrat, J.F. Joanny, P. Pincus, *J. Phys. II* 2 (1992) 1531.
- [28] J.W. Breitenbach, H. Karlinger, *Monatshefte* 80 (1949) 312.